The FASEB Journal
The Journal of the Federation of American Societies for Experimental Biology
All Articles | Submit | Subscribe | What's New | RSS

FASEB J. 2018 Jun; 32(6): 3278–3288.
Published online 2018 Jan 18.
doi: 10.1096/fj.201701124R: 10.1096/fj.201701124R

PMCID: PMC5956242
PMID: 29401608

SUMOylation regulates cytochrome P450 2E1 expression and activity in alcoholic liver disease

Maria Lauda Tomasi,[*,1] Komal Ramani,[*,2] Minjung Ryoo,[*] Carla Cossu,[*†] Andrea Floris,[*‡] Ben J. Murray,[*] Ainhoa Iglesias-Ara,[§] Ylenia Spissu,[*†] and Nirmala Mavila[*]

[*]Department of Medicine, Cedars-Sinai Medical Center, Los Angeles, California, USA;
[†]Department of Clinical and Experimental Medicine, University of Sassari, Sassari, Italy;
[‡]Department of Medical Sciences, University of Cagliari, Cagliari, Italy;
[§]Department of Genetics, Physical Anthropology and Animal Physiology, University of the Basque Country (UPV/EHU), Bilbao, Spain
[1]Correspondence: Department of Medicine, Cedars-Sinai Medical Center, DAVIS Research Building 3096A, 8700 Beverly Blvd., Los Angeles, CA 90048, USA., E-mail: marialauda.tomasi@cshs.org
[2]Correspondence: Department of Medicine, Cedars-Sinai Medical Center, DAVIS Research Building 2094, 8700 Beverly Blvd., Los Angeles, CA 90048, USA., E-mail: komal.ramani@cshs.org

Received 2017 Oct 16; Accepted 2018 Jan 8.

Abstract

Alcohol acts through numerous pathways leading to alcoholic liver disease (ALD). Cytochrome P450 (CYP2E1), an ethanol-inducible enzyme, metabolizes ethanol-producing toxic reactive oxygen species (ROS) and is regulated at the posttranslational level. Small ubiquitin-like modifier (SUMO)ylation is a posttranslational modification that involves the addition of SUMOs, which modulate protein stability, activity, and localization. We demonstrated that ubiquitin-conjugation enzyme 9, the SUMO-conjugating enzyme, is induced in the livers of an intragastric ethanol mouse model. Our aim is to examine whether SUMOylation could regulate ethanol-induced CYP2E1 expression in ALD and to elucidate the molecular mechanism(s). CYP2E1 and UBC9 expression *in vitro* and *in vivo* was detected by real-time PCR and immunoblotting/immunostaining. SUMOylation was assayed by mass spectrometry and coimmunoprecipitation. Ubc9 expression was induced in ethanol-fed mouse livers, and silencing inhibited ethanol-mediated CYP2E1 microsomal retention and enzymatic activity. CYP2E1 SUMOylation was found to be induced by ethanol *in vitro* and *in vivo*. Ubc9 silencing prevents ethanol-induced lipid accumulation and ROS production. UBC9 was highly expressed in human ALD livers. Finally, we found that lysine 410 is a key SUMOylated residue contributing to CYP2E1 protein stability and activity preventing CYP2E1 SUMOylation. Ethanol-mediated up-regulation of CYP2E1 *via* SUMOylation enhancing its protein stability and activity and may have important implications in ALD.—Tomasi, M. L., Ramani, K., Ryoo, M., Cossu, C., Floris, A., Murray, B. J., Iglesias-Ara, A., Spissu, Y., Mavila, N. SUMOylation regulates cytochrome P450 2E1 expression and activity in alcoholic liver disease.

Keywords: alcohol, CYP2E1, small ubiquitin-like modifier

Cytochrome P450 2E1 (CYP2E1) belongs to a family of heme-containing proteins that regulate the hepatic metabolism of a variety of endogenous substrates, such as steroids, fatty acids, and xenobiotics including drugs, toxins, and carcinogens (1, 2). Among the various CYP family members, CYP2E1 is characterized by its broad spectrum of substrates and generation of large amounts of reactive oxygen species (ROS),

such as the superoxide anion radical and H_2O_2, which facilitates adduct formation, activates stress proteins, induces endoplasmic reticulum stress, and affects lysosomal function and autophagy, leading to mitochondrial injury and cell death (2, 3). CYP2E1 is an inducible enzyme, and many of its substrates can induce their own metabolism. This was initially observed with ethanol. Alcohol stabilizes the enzyme by protecting it from degradation and, at higher concentrations, increases the rate of gene transcription (4, 5). During liver injury, hepatocytes are exposed to exogenous ROS produced by macrophages and neutrophils activated as part of the accompanying inflammatory reaction (2, 6). The role of CYP2E1 in hepatocyte injury has been elucidated using HepG2 cells overexpressing CYP2E1, CYP2E1 knockout mice, and transgenic mice (7). Because ethanol-activated CYP2E1 generates ROS, CYP2E1 has been suggested to play a major role in ethanol-induced oxidant stress production and in ethanol-induced liver injury development (8).

Posttranslational modification by small ubiquitin-like modifiers (SUMOs) has been identified as an important regulatory event implicated in several cellular processes, such as transcriptional regulation, protein stability, stress-induced response, cell cycle progression, and DNA repair (9). There are 4 SUMO genes (SUMO1–O4) that encode SUMO proteins distantly related to ubiquitin (10, 11). Despite a similar conjugation mechanism, ubiquitin and SUMO generally direct their targets to very different fates (12). During SUMOylation, SUMO proteins are activated by the E1-activating enzyme and then passed on to the active site cysteine residue of the E2-conjugating enzyme or the ubiquitin-conjugating enzyme 9 (UBC9), which works in conjunction with an E3 enzyme in transferring SUMO to the target protein (13). UBC9 is the sole E2-conjugating enzyme, without which SUMOylation reactions cannot occur in the cell (13). Attachment of SUMO can induce relocalization of the target protein within the cell, cause a conformational change, increase protein stability, or alter protein-protein interactions, but often its mode of action remains poorly understood (9, 14). SUMOylation has been reported to be induced by oxidative stress (15). Cellular stress arising from imbalances in genotoxic metabolites, osmolarity, and ROS are robust stimuli for protein SUMOylation (16, 17).

We previously demonstrated that the level of UBC9 is induced in the livers of intragastric ethanol-infusion–treated mice (18). However, the underlying mechanism by which dysregulated SUMOylation influences ethanol-induced liver injury development is unknown. We initially performed a proteomics analysis of SUMOylated proteins from normal and ethanol-fed mouse livers. From this screening, we identified CYP2E1 to be highly SUMOylated after ethanol exposure. The aim of the current work is to determine whether dysregulated SUMOylation could influence ethanol-induced CYP2E1 expression in alcoholic liver disease (ALD) and to elucidate the molecular mechanism(s) involved. Here, we report that ethanol-mediated up-regulation of CYP2E1 *via* SUMOylation induction leads to increased CYP2E1 protein stability and enzymatic activity. Our findings have important implications in the regulation of ethanol-induced CYP2E1 expression in ALD.

MATERIALS AND METHODS

Materials

Ethanol (200 proof), cyclohexamide, and actinomicin D were purchased from Sigma-Aldrich (St. Louis, MO, USA). H2DCFDA (2 2.9.2 2′,7′-dichlorodihydrofluorescein diacetate) was purchased from Invitrogen (Carlsbad, CA, USA). CYP2E1 recombinant protein was purchased from GenWay Biotech (San Diego, CA, USA). All other reagents were of analytical grade and obtained from commercial sources.

Cell culture and treatment

Mouse hepatocytes from 3-mo-old male C57/B6 mice were isolated by collagenase perfusion as described by the Cell Culture Core of the USC Research Center for Liver Diseases (19). Cells were plated at a density of 0.5×10^6 cells per well in 6-well plates unless indicated otherwise. Cultures were maintained in DMEM supplemented with 10% fetal calf serum, 2 mM glutamine, 50 mM penicillin, and 50 mg/ml streptomycin sulfate. After 2 h, the medium was changed to contain 2.5% fetal calf serum (20), and the hepatocytes were treated with 100 mM ethanol for 24 h. Human hepatoblastoma cell line HepG2 was purchased from American Type Culture Collection (Manassas, VA, USA) and cultured in DMEM containing 10% serum according to the manufacturer.

Human liver specimens

Three deidentified normal and 3 ALD liver tissues that were pathologically alcoholic cirrhosis were obtained through collaboration with the Internal Medicine and Liver Center at the University of Kansas Medical Center. The samples were received in frozen state and stored at −80°C until analysis.

Animal study

Three-month-old male C57/B6 mice (Harlan, Indianapolis, IN, USA) were fed a standard diet *ad libitum* (Harland irradiated mouse diet 7912; Teklad, Madison, WI, USA) and housed in a temperature-controlled animal facility with 12-h light-dark cycles. Animals were treated humanely, and all procedures complied with our institution's guidelines for the use of laboratory animals.

Mice were divided into 4 groups, with 6 mice in each group: Scrambled, EtOH treatment, siUbc9, and EtOH/siUbc9 treatment. The animals received 2 intraperitoneal injections of RNAi against Ubc9 or scrambled RNAi (once every 12 h; 100 μg small interfering RNA/mouse) (Genepharma, Shanghai, China) using LIPID-based *In Vivo* Transfection Reagent (Altogen Biosystems, Las Vegas, NV, USA). After the injections, ethanol or water was administered by oral gavage every 12 h for a total of 3 doses (5 g/kg body weight). Control mice received an isocalorical maltose solution. At 4 h after the last dose, the mice were anesthetized and euthanized, and the liver tissues were removed, snap frozen in liquid nitrogen, and stored at −80°C until analysis.

An additional ethanol-fed mouse model was used. Mouse binge ethanol–feeding liver tissue was kindly provided by Dr. Bin Gao [National Institutes of Health, National Institute on Alcohol Abuse and Alcoholism (NIAAA); Bethesda, MD, USA] (21).

RNA isolation and gene expression analysis

Total RNA isolated from primary mouse hepatocytes, HepG2 cells, and mouse liver tissues was subjected to RT by using M-MLV Reverse Transcriptase (Invitrogen) as described in Yang *et al*. (22). One microliter of RT product was subjected to quantitative real-time PCR analysis. The primers and TaqMan probes for human UBC9 and CYP2E1, murine Ubc9 and Cyp2E1, and Universal PCR Master Mix were purchased from Applied Biosystems (Foster City, CA, USA). 18SrRNA was used as housekeeping gene as described in Chen *et al*. (23). The ΔC_t obtained was used to find the relative expression of genes according to the formula: relative expression = $2^{-\Delta\Delta Ct}$, where $\Delta\Delta C_t = \Delta C_t$ of respective genes in experimental groups, ΔC_t of the same genes in control group.

Western blots and coimmunoprecipitation

Protein extracts from primary mouse hepatocytes, HepG2, and mouse livers were prepared as described in Ramani *et al*. (19) and immunoprecipitated by specific SUMO-1 antibody and processed as reported (24). Immunoprecipitated proteins were subjected to Western blotting following standard protocols (Amersham BioSciences, Piscataway, NJ, USA), and the membranes were probed with the anti-CYP2E1 antibody (Origene, Rockville, MD, USA). The Clean-Blot IP Reagent (Thermo Fisher Scientific, Waltham, MA, USA) was used to eliminate detection interference from heavy-chain (∼50 kDa) and light-chain (25 kDa) IgG fragments of antibodies used for the initial immunoprecipitation assay. Blots were developed using enhanced chemiluminescence.

Preparation of hepatic microsomes and determination of microsomal proteins

Microsomal fractions were prepared from primary mouse hepatocytes and liver homogenate using differential centrifugation as previously described (25). Pellets were resuspended in 50 mM potassium phosphate buffer (pH 7.4) and snap frozen. Levels of CYP2E1 protein were determined by Western immunoblot analysis as described previously.

SUMOylation profiling using mass spectrometry

Total proteins from control and ethanol binge mouse livers were immunoprecipitated with SUMO-1 and SUMO-2/3 antibodies using a Pierce Crosslink IP Kit (Thermo Fisher Scientific) and then separated on 10% SDS-PAGE followed by silver staining (SilverQuest Silver Staining Kit; Invitrogen). Ethanol-fed mouse protein bands between 35 and 75 KDa were submitted for mass spectrometry at the proteomics core of Cedars-Sinai Medical Center.

Overexpression of wild-type and mutant CYP2E1

Myc-DDK–tagged CYP2E1 overexpression vector (CYP2E1-pCMV6) and negative control empty vector (pCMV6) were purchased from Origene. Mutation of CYP2E1 predicted SUMO-binding Lysine site (K410) to Alanine (A410) was performed by Quick Change II Site-Directed Mutagenesis Kit (Stratagene, La Jolla, CA, USA) with pCMV6 as the template. PAGE-purified primers were synthesized by Valuegene (San Diego, CA, USA) (forward: 5′-GACTTCTGCTTCACAGAAACGCCCATCCGCAGGAATCCCAACC-3′; reverse: 5′-GGTTGGGATTCCTGCGGATGGGCGTTTCTGTGAAGCAGAAGTC-3′). HepG2 cells were cultured in 6-well plates (0.3×10^6 cells/well) and transfected using 5 µl of JetPrime (Polyplus, New York, NY, USA) with 2 µg of target plasmid per well. After 4 h, the transfection medium was changed to normal medium. The cells were cultured for an additional 20 h for mRNA and protein expression analysis as indicated.

Immunohistochemistry

Formalin-fixed liver tissues embedded in paraffin were cut and stained with hematoxylin and eosin for routine histology. Immunohistochemistry staining of CYP2E1, UBC9, and IgG was performed with a kit from Abcam (Cambridge, United Kingdom) according to the manufacturer's instructions. Control with normal mouse IgG showed no staining (not shown).

CYP2E1 activity assay

Microsomal pellets from liver and hepatocyte homogenates as described previously was resuspended in 125 mM KCl and10 mM KPi (pH 7.4). The catalytic activity of microsomal CYP2E1 was measured by the p-nitrocatechol hydroxylation method (3). The molar extinction coefficient of 9.53×10^5 M^{-1} cm^{-1} was used to calculate the amount nitrocatechol formed in the samples. Results were expressed as nanomole of product per hour per microgram of microsomal protein.

SUMO prediction and *in vitro* SUMOylation of CYP2E1

Protein sequences of human (P05181) and mouse (Q05421) CYP2E1 were aligned using Clustal Omega SUMOplot Analysis Program and GPS-SUMO (26) were used to identify possible SUMOylation sites. A search using the protein data bank (*www.rcsb.org*) was done to obtain a crystal structure of human CYP2E1 (27). Pymol was used to generate Fig. 6*B*. Recombinant CYP2E1 (1 µg) was SUMOylated *in vitro* using the SUMOylation kit (Enzo Life Sciences, Farmingdale, NY, USA) in a final volume of 10 µl containing 55 mM Tris (pH 7.5), 5.5 mM $MgCl_2$, 2.2 mM ATP, and 5.5 mM DTT. SUMOylation reactions were incubated at 37°C for 4 h, after which proteins were analyzed by Western blotting with SUMO-1 and SUMO-2/3 antibodies.

Fluorescence microscopy

For studies of the subcellular localization of CYP2E1 and SUMO-1, hepatocytes were plated at a density of 0.5×10^5 cells in a 4-well chamber slide and pretreated with collagen I for 8 h. The cells were fixed, made permeable, and processed for direct immunofluorescence microscopy by the ICC Abcam protocol (Abcam) to detect cellular CYP2E1 and SUMO-1 localization. Cells were counterstained with Vectashield mounting medium with DAPI (Vector Laboratories, Burlingame, CA, USA) and viewed by confocal microscopy.

ROS detection

To assess ROS produced by ethanol, 0.5×10^6 primary mouse hepatocytes per well were grown in 6-well plates and treated with 100 mM ethanol for 24 h in DMEM with 10% serum. After 23 h of ethanol treatment, H2DCFDA (30 μM) was added, and fluorescence intensity of the cells was detected at 485 nm excitation and 520 nm emission using confocal microscopy. Ethanol-treated mouse hepatocyte H_2O_2 concentration was measured using the ROS-Glo H_2O_2 Assay Kit (Promega, Madison, WI, USA).

Protein stability assay and half-life determination

CHX (5 μg/ml) was added to HepG2 cells after transfection with 2 μg of wild-type (WT) CYP2E1-pCMV6 or CYP2E1 SUMOylation mutant plasmids per well for 0, 12, and 24 h. Protein levels were determined at the indicated time points by Western blotting as described previously using anti-CYP2E1 antibody. The relative amount of CYP2E1-DDK protein was evaluated by densitometry and normalized to actin. Endogenous and DDK-tagged CYP2E1 bands were separately analyzed. Protein half-life was determined for each experiment using linear regression analysis as described in Tomasi *et al.* (18).

Statistical analysis

Data are expressed as means ± SEM. Statistical analysis was performed using ANOVA and Fisher's tests. For mRNA and protein levels, the ratios of genes and proteins to respective housekeeping densitometric values were compared. Significance was defined as $P < 0.05$.

RESULTS

UBC9 regulates CYP2E1 expression and cellular localization

UBC9 expression and SUMOylation are increased in response to oxidative stress (28). Ethanol-fed mouse livers exhibit increased oxidative stress and UBC9 expression (6, 18). Proteomics analysis identified CYP2E1 to be highly SUMOylated in alcohol-fed mouse livers (Supplemental Table 1). To determine whether deregulation of UBC9 by ethanol influences CYP2E1, we examined its expression in primary mouse hepatocytes. Real-time PCR analysis indicated that *Cyp2E1* and *Ubc9* mRNA levels were induced by 1.4- and 1.2-fold, respectively, upon ethanol exposure compared with control (**Fig. 1*A***). *Ubc9* knockdown did not affect the mRNA level of *Cyp2E1* (Fig. 1*A*). Because the microsomal ethanol oxidation system was shown to contain the CYP2E1 activity responsible for ethanol oxidation (29), we measured the effect of *Ubc9* silencing on microsomal CYP2E1 protein level and cellular localization (Fig. 1*B*). Ethanol treatment increases microsomal the CYP2E1 protein level by 3.1-fold compared with control, whereas nonmicrosomal CYP2E1 is induced marginally by 1.3-fold after ethanol treatment (Fig. 1*B*). Knockdown of *Ubc9* inhibited CYP2E1 protein level by 60% compared with control in the microsome and correspondingly raised the nonmicrosomal CYP2E1 by 3-fold compared with control, indicating that UBC9 was required to retain CYP2E1 in the microsome. Ethanol was less efficient in retaining microsomal CYP2E1 in cells lacking *Ubc9* (1.8-fold in ethanol + *siUbc9 vs.* 3-fold in ethanol alone) (Fig. 1*B*), indicating that ethanol-mediated CYP2E1 microsomal accumulation was enhanced by UBC9 or SUMOylation. Although the knockdown efficiency of *Ubc9* was 90% in both microsomal and nonmicrosomal fractions, ethanol treatment appeared to retain more microsomal UBC9 protein even under conditions of *Ubc9* silencing (Fig. 1*B*).

UBC9 regulates ethanol-mediated ROS production

Because ethanol-mediated CYP2E1 induction is a key mechanism to produce toxic metabolites and ROS (3), we measured ROS production upon *Ubc9* silencing in the presence of ethanol. Based on bioluminescent assay, we measured the level of H_2O_2, an endogenous ROS form, and demonstrated that *Ubc9* silencing prevents ethanol-induced ROS production (Fig. 1*C*). The nonfluorescent H2DCFDA probe was used to measure the oxidative stress level in cells by its conversion to the highly fluorescent 2′,7′-dichlorofluorescein, and we found that UBC9 expression is required by ethanol to induce ROS production (Fig. 1*D*). We also found that *Ubc9* silencing protects against ethanol-induced triglyceride accumulation (Fig. 1*E*).

CYP2E1 is SUMOylated by SUMO-1

Posttranslational stabilization of CYP2E1 is the principle mechanism for induction by most xenobiotics and is one of the main mechanisms of CYP2E1 regulation (30). Our results show that *Ubc9* knockdown lowers CYP2E1 protein level in primary mouse hepatocytes (Fig. 1*B*). SUMOylation by SUMO-1 has been shown to control protein stability of protein target (31). Using SUMOplot, SUMOsp2.0, and GSP-SUMO-1 SUMOylation prediction software, we identified 4 highly scored potential SUMOylated sites (K317, K342, K410, and K428) on the CYP2E1 protein sequence (**Table 1**). To investigate whether CYP2E1 is SUMOylated *in vitro*, we carried out *in vitro* SUMOylation assays using highly purified CYP2E1 recombinant protein and a commercially available SUMOylation Assay Kit (32). SUMOylated proteins have been found showing higher MW compared with their non-SUMOylated counterparts (33). **Figure 2*A*** shows that recombinant CYP2E1 is SUMOylated by SUMO-1, SUMO-2, and SUMO-3. CYP2E1 was preferentially modified by SUMO-1, showing 5 slower migrating forms instead of 3 and 1 by SUMO-2 and SUMO-3, respectively. Figure 2*B* shows differentially silver-stained bands whose expression resulted in increased microsomal proteins from ethanol-fed *vs.* control mouse liver. Collected gel bands from 35 to 75 KDa were analyzed by mass spectrometry, and CYP2E1 was identified as SUMOylated only by SUMO-1 (Supplemental Table 1). Additional evidence of CYP2E1 SUMOylation by SUMO-1 was provided by coimmunoprecipitation analysis in primary human and mouse hepatocytes (Fig. 2*C*). Colocalization of SUMO-1 and CYP2E1 was observed in mouse hepatocytes by confocal microscopy (Fig. 2*D*).

SUMOylation regulates CYP2E1 protein trafficking in ethanol-fed mice

As expected, CYP2E1 and UBC9 proteins were induced in the liver of the NIAAA ethanol-binge model compared with pair-fed controls (**Fig. 3*A***). To investigate whether SUMOylation plays a role in CYP2E1 cellular trafficking *in vivo*, we measured the conjugation level of CYP2E1 with SUMO-1 in microsomal and nonmicrosomal compartments. Compared with WT mice, ethanol-fed mice exhibited higher SUMOylated and total CYP2E1 in the microsomal fraction. However, the ratio of SUMOylated form to total CYP2E1 in the microsomes was significantly higher in the ethanol groups compared with control (Fig. 3*B*). On the other hand, SUMOylated CYP2E1 fell drastically in ethanol-fed mice in nonmicrosomal compartments compared with control (Fig. 3*B*).

UBC9 regulates CYP2E1 expression and triglyceride accumulation in acute ethanol-fed mice

We next investigated whether CYP2E1 protein sustenance during ethanol feeding was dependent on its SUMOylation status in the liver. **Figure 4*A*, *B*** shows that silencing of *Ubc9* prevents ethanol-mediated induction of liver CYP2E1 protein levels. In addition, *Ubc9* knockdown blocks ethanol-induced fat accumulation (Fig. 4*A*). Using this acute model, we were able to confirm the role of SUMOylation in CYP2E1 microsomal retention observed *in vitro* (Fig. 1*B*). These results suggest that Ubc9-mediated SUMOylation of CYP2E1 may contribute to higher CYP2E1 protein levels during ethanol feeding. Moreover, CYP2E1 activity was induced 1.73-fold by ethanol compared with control and was completely inhibited when *Ubc9* was silenced (Fig. 4*C*).

UBC9 is overexpressed in human ALD specimens

We investigated the correlation between CYP2E1 expression and UBC9 in human liver samples from patients with ALD. Five liver samples from patients with ALD and 5 liver samples from normal patients exhibited a 2.2-fold induction in CYP2E1 protein compared with normal (**Fig. 5*A*, *C***) despite a drop in mRNA level (Fig. 5*B*). This finding was confirmed using the Gene Expression Omnibus Profiles database in human alcoholic hepatitis (National Center for Biotechnology Information, Bethesda, MD, USA; *https://www.ncbi.nlm.nih.gov/geo/tools/profileGraph.cgi?ID=GDS4389:209976_s_at*). UBC9 mRNA and protein were induced by 1.6- and 2.7-fold, respectively, compared with normal (Fig. 5).

SUMOylation of K410 is critical for CYP2E1 protein stability and activity in HepG2 cells

A sequence alignment of mouse and human CYP2E1 reveals that 3 of the 4 lysine residues are conserved between the 2 species, with the exception of K342 (**Fig. 6*A***). Only K410 contains the classic SUMOylation site sequence Ψ-K-*x*-E, where ψ is a bulky aliphatic amino acid and *x* is any residue (Fig. 6*A*). Visualizing the candidate residues on the 3-dimensional crystal structure of CYP2E1 shows that

all 4 lysine are located on the surface of the protein and are accessible to modification (Fig. 6*B*). A closer view of K317 and K342 shows that both are situated on α helical structures (which are not suited for SUMOylation), whereas K410 and K428 lie on unstructured areas (Fig. 6*B*). Because knockdown of *Ubc9* lowered the CYP2E1 protein level (Figs. 1*B* and 4*B*), we examine whether the predicted SUMO binding site (Table 1) at lysine 410 is critical for SUMO-1–regulated CYP2E1 protein stability in HepG2 cells. For this purpose, we created a mutation in the overexpression vector hCYP2E1 DDK tagged at K410 (to A410) and examined the total CYP2E1 protein level using Western blot analysis. Mutation of K410 to A410 did not affect the mRNA level of the mutant compared with WT (Fig. 6*C*). Figure 6*D* shows that mutation at K410 resulted in a less stable CYP2E1, as demonstrated by measurement of protein half-life in HepG2 cells. Moreover, we confirmed that mutated CYP2E1 A410 cannot be immunoprecipitated and SUMOylated by SUMO-1 compared with WT (Fig. 6*E*). However, overexpression of the K410A mutant caused a 40% reduction in CYP2E1 activity compared with WT CYP2E1 in HepG2 cells (Fig. 6*F*).

DISCUSSION

It is well known that the level of CYP2E1 expression is regulated at all stages of protein biosynthesis from the initiation of transcription to the posttranslational stabilization of this enzyme (34). Posttranslational substrate-dependent stabilization is one of the main mechanisms that regulates the intracellular amount of CYP2E1 (34, 35). It has been shown that the stabilization of CYP2E1 by ethanol increases its half-life from 6 to 37 h (36). Binding of a ligand to the active site of CYP2E1 protects the protein from degradation, allowing it to accumulate as a consequence of unaltered synthesis (37). It is believed that substrates, while in the active site of enzyme, change and stabilize protein structure, thus preventing its fast degradation with proteasomes (30). SUMOylation plays a major role in regulating protein stability, localization, protein-protein interaction, and enzymatic activity (9, 12). We recently demonstrated that UBC9 is induced in an intragastric ethanol–fed mouse model (18). However, the functional significance of this finding remains unknown. Many SUMOylated proteins have been identified in the liver after ethanol administration and other injury models. A notable example is the enzyme methionine adenosyltransferase II α (MATα2), which has been shown to increase upon ethanol exposure (38), is SUMOylated. This modification likely plays a critical role in its stability (39–41).

In this study, we report that the SUMOylation regulates CYP2E1 expression. Using primary mouse hepatocytes, we found that knockdown of *Ubc9* lowered CYP2E1 protein expression. In this work, we have examined SUMOylation as a mechanism for stabilizing CYP2E1. SUMOylation is commonly associated with changes in subcellular localization (42). Here, we show that UBC9-mediated SUMOylation is responsible for retaining CYP2E1 in the microsomal fraction and that ethanol-mediated microsomal retention of CYP2E1 is facilitated by its SUMOylation. Further confirmation of microsomal retention of CYP2E1 comes from our colocalization studies showing UBC9 and CYP2E1 to be colocalized. *In vivo* analysis of total liver clearly establishes that the ratio of SUMOylated CYP2E1 to total protein is significantly higher in the microsomal fraction of ethanol-fed livers compared with control. Induction of CYP2E1 by ethanol is a key mechanism by which it induces oxidative stress *via* the production of toxic metabolites and ROS (3). Ubc9 knockdown in primary mouse hepatocytes prevents ethanol-induced ROS level blocking the oxidation of H2DCFDA on 2′,7′-dichlorofluorescein and the hydrogen peroxide production, suggesting that aberrant SUMOylation signaling is evoked by oxidative stress. Also, it has been clearly demonstrated that CYP2E1 promotes lipid accumulation and is responsible for experimental alcoholic fatty liver in mice (43). Because CYP2E1 and lipid accumulation are clearly correlated, we examined whether SUMOylation was responsible for ethanol-mediated lipid accumulation and CYP2E1 induction. *In vivo Ubc9* silencing in mice clearly demonstrated that UBC9 not only promoted ethanol-mediated CYP2E1 induction but was also required for ethanol-mediated lipid accumulation in the liver. The correlation between UBC9, CYP2E1, and lipid accumulation was also observed in livers of patients with ALD.

Mapping possible SUMOylation sites onto the structure of human CYP2E1 provided a tool whereby candidate residues could be further selected not just based on sequence but also on position within the 3-dimensional structure. All 4 possible SUMOylation sites (K317, K342, K410, and K428) are located on the surface of the protein and are accessible for modification, but K410 was the only candidate on CYP2E1 that adhered to the classic SUMO motif Ψ-K-*x*-E, where ψ is a bulky aliphatic amino acid and *x* is any residue (Fig. 6*A*, *B*). UBC9 is unable to recognize the SUMO motif on a target protein if it is located

in stable helical structure (44). Two of the predicted SUMOylated residues, K317 and K342, form parts of α helical structures. Due to these findings and the fact that these lysine residues lack the complete SUMO motif, they were not pursued for experimental analysis. Also, K342 was not conserved between mouse and human. It has been shown that UBC9 recognition of a consensus site motif is only possible if the lysine residue is located as part of an unstructured region or extended loop (45, 46), and K410 and K428 reside on extended loop regions. K410 was selected as the candidate residue to pursue because it is located in an extended loop and satisfies the SUMO motif. The other predicted residues lacked the E residue of the motif and were not used for further analysis. Our mutagenesis studies demonstrated that the K410 SUMOylation site contributes to CYP2E1 stabilization and promotes its activity.

Our cumulative results identify SUMOylation of the K410 site of CYP2E1 as a novel mechanism that stabilizes microsomal CYP2E1 and enhances its activity during ethanol exposure. Based on our *Ubc9* silencing analysis, it appears that SUMO-conjugated CYP2E1 may be highly potent in facilitating ethanol-induced liver injury and hence serve as a potential therapeutic target.

Supplementary Material

This article includes supplemental data. Please visit *http://www.fasebj.org* to obtain this information.

ACKNOWLEDGMENTS

The authors thank Dr. Shelly Lu (Cedars-Sinai Medical Center) for mentoring support, Dr. Bin Gao [U.S. National Institutes of Health/National Institute on Alcohol Abuse and Alcoholism (NIH/NIAAA)] for material support, and all current and previous laboratory members for technical support and helpful discussions. This work was supported by NIH/NIAAA Grant K01AA022372 (to M.L.T.). The authors declare no conflicts of interest.

Glossary

ALD	alcoholic liver disease
CYP2E1	cytochrome P450
NIAAA	National Institute on Alcohol Abuse and Alcoholism
SUMO	small ubiquitin-like modifier
UBC9	ubiquitin-conjugating enzyme 9
ROS	reactive oxygen species
WT	wild type

Footnotes

This article includes supplemental data. Please visit *http://www.fasebj.org* to obtain this information.

AUTHOR CONTRIBUTIONS

M. L. Tomasi and K. Ramani designed the experiments, analyzed the data, and wrote the paper; M. Ryoo, C. Cossu, A. Floris, A. Iglesias-Ara, Y. Spissu, and N. Mavila performed the research; and B. J. Murray contributed analytic tools.

REFERENCES

1. Guengerich F. P. (1987) Oxidative cleavage of carboxylic esters by cytochrome P-450. J. Biol. Chem. 262, 8459–8462 [PubMed: 3597381]

2. Leung T. M., , Nieto N. (2013) CYP2E1 and oxidant stress in alcoholic and non-alcoholic fatty liver disease. J. Hepatol. 58, 395–398 10.1016/j.jhep.2012.08.018 [PubMed: 22940046] [CrossRef: 10.1016/j.jhep.2012.08.018]

3. Cederbaum A. I. (2014) Methodology to assay CYP2E1 mixed function oxidase catalytic activity and its induction. Redox Biol. 2, 1048–1054 10.1016/j.redox.2014.09.007 [PMCID: PMC4297943] [PubMed: 25454746] [CrossRef: 10.1016/j.redox.2014.09.007]

4. Lieber C. S. (1997) Cytochrome P-4502E1: its physiological and pathological role. Physiol. Rev. 77, 517–544 10.1152/physrev.1997.77.2.517 [PubMed: 9114822] [CrossRef: 10.1152/physrev.1997.77.2.517]

5. Ingelman-Sundberg M. (2004) Human drug metabolising cytochrome P450 enzymes: properties and polymorphisms. Naunyn Schmiedebergs Arch. Pharmacol. 369, 89–104 10.1007/s00210-003-0819-z [PubMed: 14574440] [CrossRef: 10.1007/s00210-003-0819-z]

6. Lu Y., , Wu D., , Wang X., , Ward S. C., , Cederbaum A. I. (2010) Chronic alcohol-induced liver injury and oxidant stress are decreased in cytochrome P4502E1 knockout mice and restored in humanized cytochrome P4502E1 knock-in mice. Free Radic. Biol. Med. 49, 1406–1416 10.1016/j.freeradbiomed.2010.07.026 [PMCID: PMC2975513] [PubMed: 20692331] [CrossRef: 10.1016/j.freeradbiomed.2010.07.026]

7. Cederbaum A. I., , Wu D., , Mari M., , Bai J. (2001) CYP2E1-dependent toxicity and oxidative stress in HepG2 cells. Free Radic. Biol. Med. 31, 1539–1543 10.1016/S0891-5849(01)00743-2 [PubMed: 11744327] [CrossRef: 10.1016/S0891-5849(01)00743-2]

8. Schattenberg J. M., , Czaja M. J. (2014) Regulation of the effects of CYP2E1-induced oxidative stress by JNK signaling. Redox Biol. 3, 7–15 10.1016/j.redox.2014.09.004 [PMCID: PMC4218941] [PubMed: 25462060] [CrossRef: 10.1016/j.redox.2014.09.004]

9. Dasso M. (2008) Emerging roles of the SUMO pathway in mitosis. Cell Div. 3, 5 10.1186/1747-1028-3-5 [PMCID: PMC2265688] [PubMed: 18218095] [CrossRef: 10.1186/1747-1028-3-5]

10. Geiss-Friedlander R., , Melchior F. (2007) Concepts in sumoylation: a decade on. Nat. Rev. Mol. Cell Biol. 8, 947–956 10.1038/nrm2293 [PubMed: 18000527] [CrossRef: 10.1038/nrm2293]

11. Becker J., , Barysch S. V., , Karaca S., , Dittner C., , Hsiao H. H., , Berriel Diaz M., , Herzig S., , Urlaub H., , Melchior F. (2013) Detecting endogenous SUMO targets in mammalian cells and tissues. Nat. Struct. Mol. Biol. 20, 525–531 10.1038/nsmb.2526 [PubMed: 23503365] [CrossRef: 10.1038/nsmb.2526]

12. Gill G. (2004) SUMO and ubiquitin in the nucleus: different functions, similar mechanisms? Genes Dev. 18, 2046–2059 10.1101/gad.1214604 [PubMed: 15342487] [CrossRef: 10.1101/gad.1214604]

13. Wilkinson K. A., , Henley J. M. (2010) Mechanisms, regulation and consequences of protein SUMOylation. Biochem. J. 428, 133–145 10.1042/BJ20100158 [PMCID: PMC3310159] [PubMed: 20462400] [CrossRef: 10.1042/BJ20100158]

14. Papouli E., , Chen S., , Davies A. A., , Huttner D., , Krejci L., , Sung P., , Ulrich H. D. (2005) Crosstalk between SUMO and ubiquitin on PCNA is mediated by recruitment of the helicase Srs2p. Mol. Cell 19, 123–133 10.1016/j.molcel.2005.06.001 [PubMed: 15989970] [CrossRef: 10.1016/j.molcel.2005.06.001]

15. Sahin U., , de Thé H., , Lallemand-Breitenbach V. (2014) PML nuclear bodies: assembly and oxidative stress-sensitive sumoylation. Nucleus 5, 499–507 10.4161/19491034.2014.970104 [PMCID: PMC4615786] [PubMed: 25482067] [CrossRef: 10.4161/19491034.2014.970104]

16. Saitoh H., , Hinchey J. (2000) Functional heterogeneity of small ubiquitin-related protein modifiers SUMO-1 versus SUMO-2/3. J. Biol. Chem. 275, 6252–6258 10.1074/jbc.275.9.6252 [PubMed: 10692421] [CrossRef: 10.1074/jbc.275.9.6252]

17. Pandey D., , Chen F., , Patel A., , Wang C. Y., , Dimitropoulou C., , Patel V. S., , Rudic R. D., , Stepp D. W., , Fulton D. J. (2011) SUMO1 negatively regulates reactive oxygen species production from NADPH oxidases. Arterioscler. Thromb. Vasc. Biol. 31, 1634–1642 10.1161/ATVBAHA.111.226621 [PMCID: PMC3464053] [PubMed: 21527745] [CrossRef: 10.1161/ATVBAHA.111.226621]

18. Tomasi M. L., , Tomasi I., , Ramani K., , Pascale R. M., , Xu J., , Giordano P., , Mato J. M., , Lu S. C. (2012) S-adenosyl methionine regulates ubiquitin-conjugating enzyme 9 protein expression and sumoylation in murine liver and human cancers. Hepatology 56, 982–993 10.1002/hep.25701 [PMCID: PMC3378793] [PubMed: 22407595] [CrossRef: 10.1002/hep.25701]

19. Ramani K., , Yang H., , Xia M., , Ara A. I., , Mato J. M., , Lu S. C. (2008) Leptin's mitogenic effect in human liver cancer cells requires induction of both methionine adenosyltransferase 2A and 2beta. Hepatology 47, 521–531 10.1002/hep.22064 [PMCID: PMC2387125] [PubMed: 18041713] [CrossRef: 10.1002/hep.22064]

20. García-Trevijano E. R., , Latasa M. U., , Carretero M. V., , Berasain C., , Mato J. M., , Avila M. A. (2000) S-adenosylmethionine regulates MAT1A and MAT2A gene expression in cultured rat hepatocytes: a new role for S-adenosylmethionine in the maintenance of the differentiated status of the liver. FASEB J. 14, 2511–2518 10.1096/fj.00-0121com [PubMed: 11099469] [CrossRef: 10.1096/fj.00-0121com]

21. Bertola A., , Mathews S., , Ki S. H., , Wang H., , Gao B. (2013) Mouse model of chronic and binge ethanol feeding (the NIAAA model). Nat. Protoc. 8, 627–637 10.1038/nprot.2013.032 [PMCID: PMC3788579] [PubMed: 23449255] [CrossRef: 10.1038/nprot.2013.032]

22. Yang H., , Ara A. I., , Magilnick N., , Xia M., , Ramani K., , Chen H., , Lee T. D., , Mato J. M., , Lu S. C. (2008) Expression pattern, regulation, and functions of methionine adenosyltransferase 2beta splicing variants in hepatoma cells. Gastroenterology 134, 281–291 10.1053/j.gastro.2007.10.027 [PMCID: PMC2409110] [PubMed: 18045590] [CrossRef: 10.1053/j.gastro.2007.10.027]

23. Chen H., , Xia M., , Lin M., , Yang H., , Kuhlenkamp J., , Li T., , Sodir N. M., , Chen Y. H., , Josef-Lenz H., , Laird P. W., , Clarke S., , Mato J. M., , Lu S. C. (2007) Role of methionine adenosyltransferase 2A and S-adenosylmethionine in mitogen-induced growth of human colon cancer cells. Gastroenterology 133, 207–218 10.1053/j.gastro.2007.03.114 [PubMed: 17631143] [CrossRef: 10.1053/j.gastro.2007.03.114]

24. Pascale R. M., , Simile M. M., , De Miglio M. R., , Muroni M. R., , Calvisi D. F., , Asara G., , Casabona D., , Frau M., , Seddaiu M. A., , Feo F. (2002) Cell cycle deregulation in liver lesions of rats with and without genetic predisposition to hepatocarcinogenesis. Hepatology 35, 1341–1350 10.1053/jhep.2002.33682 [PubMed: 12029619] [CrossRef: 10.1053/jhep.2002.33682]

25. Murray M., , Zaluzny L., , Farrell G. C. (1986) Drug metabolism in cirrhosis. Selective changes in cytochrome P-450 isozymes in the choline-deficient rat model. Biochem. Pharmacol. 35, 1817–1824 10.1016/0006-2952(86)90298-4 [PubMed: 3718530] [CrossRef: 10.1016/0006-2952(86)90298-4]

26. Zhao Q., , Xie Y., , Zheng Y., , Jiang S., , Liu W., , Mu W., , Liu Z., , Zhao Y., , Xue Y., , Ren J. (2014) GPS-SUMO: a tool for the prediction of sumoylation sites and SUMO-interaction motifs. Nucleic Acids Res. 42, W325–W330 10.1093/nar/gku383 [PMCID: PMC4086084] [PubMed: 24880689] [CrossRef: 10.1093/nar/gku383]

27. Porubsky P. R., , Battaile K. P., , Scott E. E. (2010) Human cytochrome P450 2E1 structures with fatty acid analogs reveal a previously unobserved binding mode. J. Biol. Chem. 285, 22282–22290 10.1074/jbc.M110.109017 [PMCID: PMC2903405] [PubMed: 20463018] [CrossRef: 10.1074/jbc.M110.109017]

28. Romanenko A. M., , Kinoshita A., , Wanibuchi H., , Wei M., , Zaparin W. K., , Vinnichenko W. I., , Vozianov A. F., , Fukushima S. (2006) Involvement of ubiquitination and sumoylation in bladder lesions induced by persistent long-term low dose ionizing radiation in humans. J. Urol. 175, 739–743 10.1016/S0022-5347(05)00172-2 [PubMed: 16407042] [CrossRef: 10.1016/S0022-5347(05)00172-2]

29. Lieber C. S. (1999) Microsomal ethanol-oxidizing system (MEOS): the first 30 years (1968-1998)--a review. Alcohol. Clin. Exp. Res. 23, 991–1007 [PubMed: 10397283]

30. Bardag-Gorce F., , Yuan Q. X., , Li J., , French B. A., , Fang C., , Ingelman-Sundberg M., , French S. W. (2000) The effect of ethanol-induced cytochrome p4502E1 on the inhibition of proteasome activity by alcohol. Biochem. Biophys. Res. Commun. 279, 23–29 10.1006/bbrc.2000.3889 [PubMed: 11112412] [CrossRef: 10.1006/bbrc.2000.3889]

31. Klenk C., , Humrich J., , Quitterer U., , Lohse M. J. (2006) SUMO-1 controls the protein stability and the biological function of phosducin. J. Biol. Chem. 281, 8357–8364 10.1074/jbc.M513703200 [PubMed: 16421094] [CrossRef: 10.1074/jbc.M513703200]

32. Elmore Z. C., , Donaher M., , Matson B. C., , Murphy H., , Westerbeck J. W., , Kerscher O. (2011) Sumo-dependent substrate targeting of the SUMO protease Ulp1. BMC Biol. 9, 74 10.1186/1741-7007-9-74 [PMCID: PMC3216068] [PubMed: 22034919] [CrossRef: 10.1186/1741-7007-9-74]

33. Stielow C., , Stielow B., , Finkernagel F., , Scharfe M., , Jarek M., , Suske G. (2014) SUMOylation of the polycomb group protein L3MBTL2 facilitates repression of its target genes. Nucleic Acids Res. 42, 3044–3058 10.1093/nar/gkt1317 [PMCID: PMC3950706] [PubMed: 24369422] [CrossRef: 10.1093/nar/gkt1317]

34. Ingelman-Sundberg M., , Ronis M. J., , Lindros K. O., , Eliasson E., , Zhukov A. (1994) Ethanol-inducible cytochrome P4502E1: regulation, enzymology and molecular biology. Alcohol Alcohol. Suppl. 2, 131–139 [PubMed: 8974327]

35. Song B. J., , Veech R. L., , Park S. S., , Gelboin H. V., , Gonzalez F. J. (1989) Induction of rat hepatic N-nitrosodimethylamine demethylase by acetone is due to protein stabilization. J. Biol. Chem. 264, 3568–3572 [PubMed: 2914964]

36. Zanelli U., , Longo V., , Paolicchi A., , Gervasi P. G. (2000) Stabilization of cytochrome P4502E1 protein by ethanol in primary hamster hepatocyte cultures. Toxicol. In Vitro 14, 69–77 10.1016/S0887-2333(99)00085-5 [PubMed: 10699363] [CrossRef: 10.1016/S0887-2333(99)00085-5]

37. Chien J. Y., , Thummel K. E., , Slattery J. T. (1997) Pharmacokinetic consequences of induction of CYP2E1 by ligand stabilization. Drug Metab. Dispos. 25, 1165–1175 [PubMed: 9321520]

38. Tsukamoto H., , Lu S. C. (2001) Current concepts in the pathogenesis of alcoholic liver injury. FASEB J. 15, 1335–1349 10.1096/fj.00-0650rev [PubMed: 11387231] [CrossRef: 10.1096/fj.00-0650rev]

39. Tomasi M. L., , Ryoo M., , Ramani K., , Tomasi I., , Giordano P., , Mato J. M., , Lu S. C. (2015) Methionine adenosyltransferase α2 sumoylation positively regulate Bcl-2 expression in human colon and liver cancer cells. Oncotarget 6, 37706–37723 10.18632/oncotarget.5342 [PMCID: PMC4741959] [PubMed: 26416353] [CrossRef: 10.18632/oncotarget.5342]

40. He L., , Ronis M. J., , Badger T. M. (2002) Ethanol induction of class I alcohol dehydrogenase expression in the rat occurs through alterations in CCAAT/enhancer binding proteins beta and gamma. J. Biol. Chem. 277, 43572–43577 10.1074/jbc.M204535200 [PubMed: 12213809] [CrossRef: 10.1074/jbc.M204535200]

41. Davis R. L., , Syapin P. J. (2004) Acute ethanol exposure modulates expression of inducible nitric-oxide synthase in human astroglia: evidence for a transcriptional mechanism. Alcohol 32, 195–202 10.1016/j.alcohol.2004.01.006 [PubMed: 15282113] [CrossRef: 10.1016/j.alcohol.2004.01.006]

42. Carter S., , Vousden K. H. (2008) p53-Ubl fusions as models of ubiquitination, sumoylation and neddylation of p53. Cell Cycle 7, 2519–2528 10.4161/cc.7.16.6422 [PubMed: 18719371] [CrossRef: 10.4161/cc.7.16.6422]

43. Lu Y., , Zhuge J., , Wang X., , Bai J., , Cederbaum A. I. (2008) Cytochrome P450 2E1 contributes to ethanol-induced fatty liver in mice. Hepatology 47, 1483–1494 10.1002/hep.22222 [PubMed: 18393316] [CrossRef: 10.1002/hep.22222]

44. Pichler A., , Knipscheer P., , Oberhofer E., , van Dijk W. J., , Körner R., , Olsen J. V., , Jentsch S., , Melchior F., , Sixma T. K. (2005) SUMO modification of the ubiquitin-conjugating enzyme E2-25K. Nat. Struct. Mol. Biol. 12, 264–269 10.1038/nsmb903 [PubMed: 15723079] [CrossRef: 10.1038/nsmb903]

45. Macauley M. S., , Errington W. J., , Schärpf M., , Mackereth C. D., , Blaszczak A. G., , Graves B. J., , McIntosh L. P. (2006) Beads-on-a-string, characterization of ETS-1 sumoylated within its flexible N-terminal sequence. J. Biol. Chem. 281, 4164–4172 10.1074/jbc.M510488200 [PubMed: 16319071] [CrossRef: 10.1074/jbc.M510488200]

46. Bernier-Villamor V., , Sampson D. A., , Matunis M. J., , Lima C. D. (2002) Structural basis for E2-mediated SUMO conjugation revealed by a complex between ubiquitin-conjugating enzyme Ubc9 and RanGAP1. Cell 108, 345–356 10.1016/S0092-8674(02)00630-X [PubMed: 11853669] [CrossRef: 10.1016/S0092-8674(02)00630-X]

Figures and Tables

Figure 1.

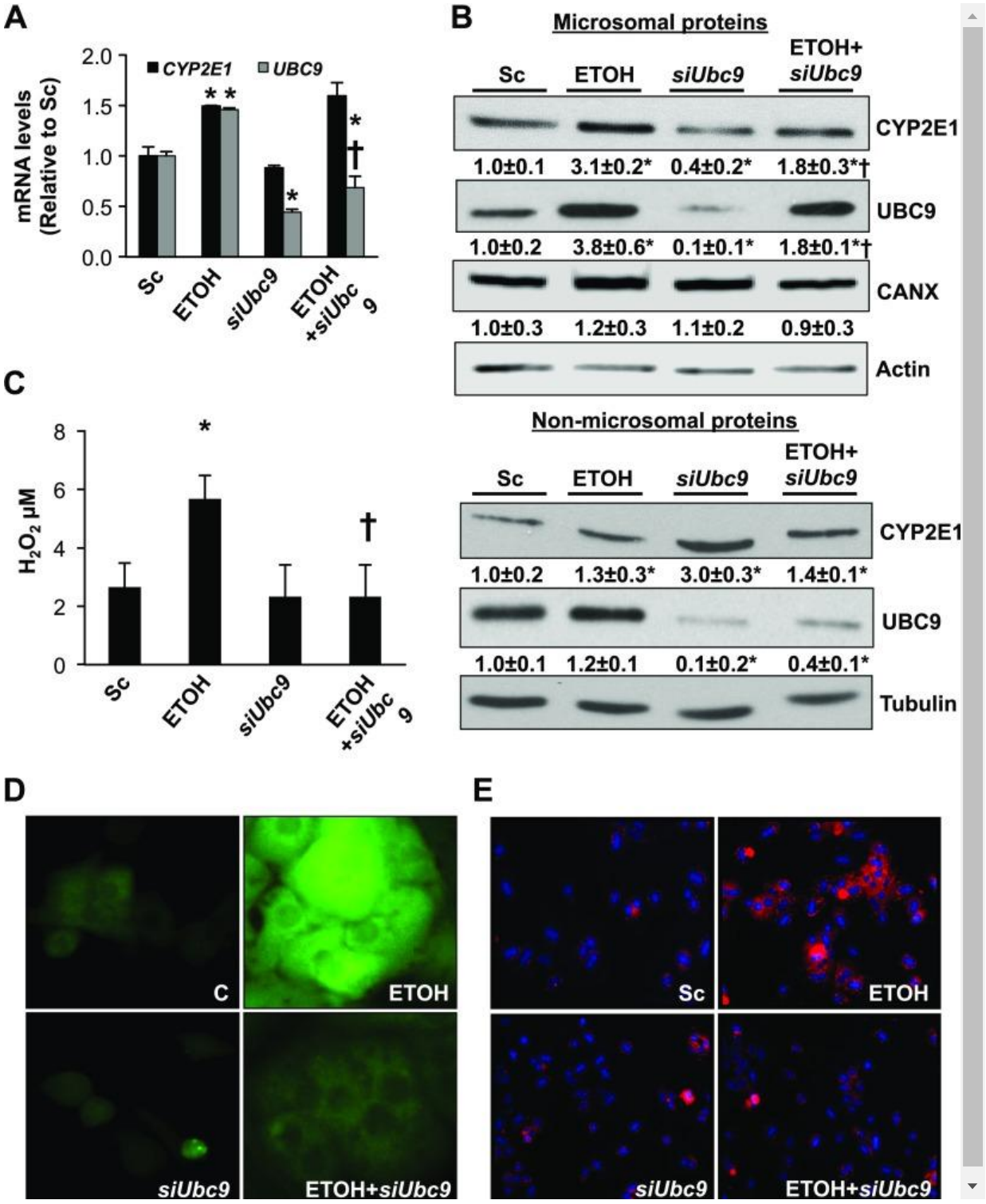

Open in a separate window

UBC9 regulates CYP2E1 protein level and cellular localization modulating ethanol-induced ROS production. Mouse hepatocytes were plated at a density of 0.5×10^6 cells per well in 6-well plates and transfected with *siUbc9* (10 nM) or scrambled small interfering RNA (Sc) for 48 h and/or treated with ethanol (100 mM) for the last 24 h. *A*) The mRNA levels of *Cyp2E1* and *Ubc9* were compared with Sc using real-time PCR. Results represent mean ± SE from 3 experiments in duplicate. $^*P < 0.04$ *vs.* Sc, $^\dagger P < 0.03$ *vs.* ethanol. *B*) Western blotting of microsomal fractions and nonmicrosomal components. Results are expressed as fold of Sc (mean ± SE) from 3 independent experiments. $^*P < 0.03$ *vs.* Sc, $^\dagger P < 0.05$ *vs.* ethanol. *C*) Hydrogen peroxide was measured by bioluminescence reading. Values are expressed as means ± SEM ($n = 3$). $^*P < 0.02$ *vs.* Sc, $^\dagger P < 0.02$ *vs.* ethanol. *D*, *E*) Hepatocytes treated with 100 mM ethanol for 24 h were incubated with H2DCFDA or Nile Red for 30 min to detect ROS and triglycerides production, respectively.

TABLE 1.

SUMOylation prediction of CYP2E1

Prediction software	Sites (*n*)	Position	Site name
GPS-SUMO 1.0	4	17–21	LLVWAAF*LLLVS*MWRQVHS
		237	GSHRKVI*K*NVAEVKE
		312–316	STTLRYG*LLILM*KYPEIEE
		410	FPDPEKF*K*PEHFLNE
SUMOsp 2.0	2	342	PAI*K*DRQ
		410	EKF*K*PEH
SUMOplot	6	415	PDPEK *FKPE*HFLNE
		321	GLLIL*MKYP*EIEEK
		434	KYSDY*FKPF*STGKR
		425	FLNEN*GKF*KYSDY
		55	ELKNI*PKSF*TRLAQ
		189	ADILF*RKHF*DYNDE
PCI SUMO	6	87	VMHGYKAV*K*EALLDYKD
		342	GPSRIPAI*K*DRQEMPYM
		410	EFPDP*EKFKPE*HFLNEN
		422	FLNENGKF*K*YSDYFKPF
		428	KFKYSDYF*K*PFSTGKRV
		467	NLKPLVDP*K*DIDLSPIH

Open in a separate window

Predicted SUMO binding site sequences are italic and underlined.

Figure 2.

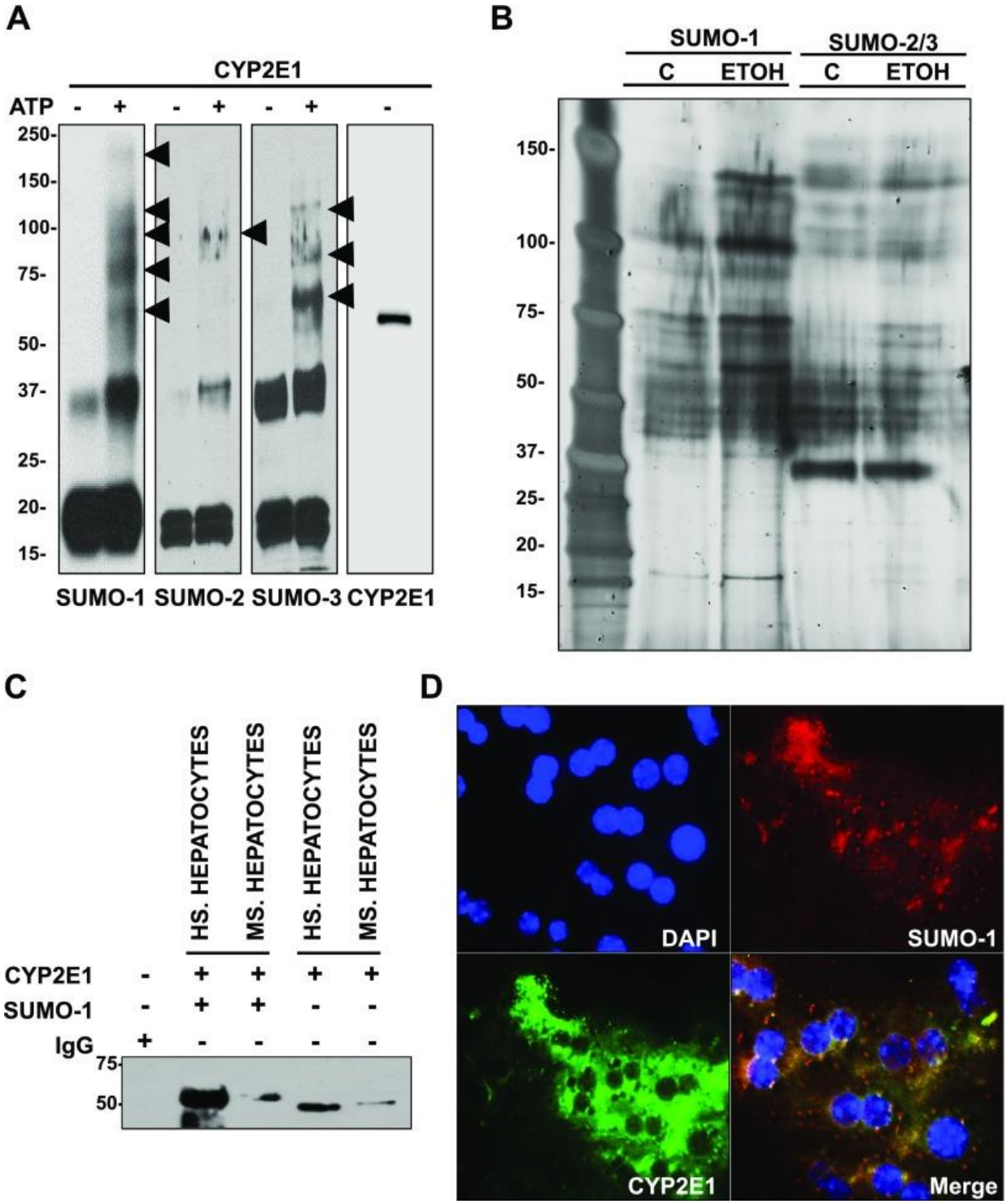

Open in a separate window

CYP2E1 is SUMOylated by SUMO-1. *A*) SUMOylation of CYP2E1 by SUMO-1, SUMO-2, and SUMO-3 recombinant protein system. SUMOylation was measured using anti–SUMO-1, anti–SUMO-2, and anti–SUMO-2 antibodies in Western blotting. Black arrows indicate SUMOylated CYP2E1. *B*) Liver microsomal proteins were immunoprecipitated by SUMO-1 and SUMO-2/3 antibodies and separated by 10% SDS-PAGE. The protein bands were detected in the gels by silver staining. *C*) SUMOylation of CYP2E1 in human and mouse primary hepatocytes. Protein was extracted, and 700 μg of cell extracts were used to immunoprecipitate SUMO-1 and then loaded on 12% SDS-PAGE followed by Western blot against CYP2E1. *D*) Confocal microscopy of CYP2E1 and SUMO-1 colocalization. CYP2E1 and SUMO-1 proteins appear green and red, respectively, on fluorescence microscopy.

Figure 3.

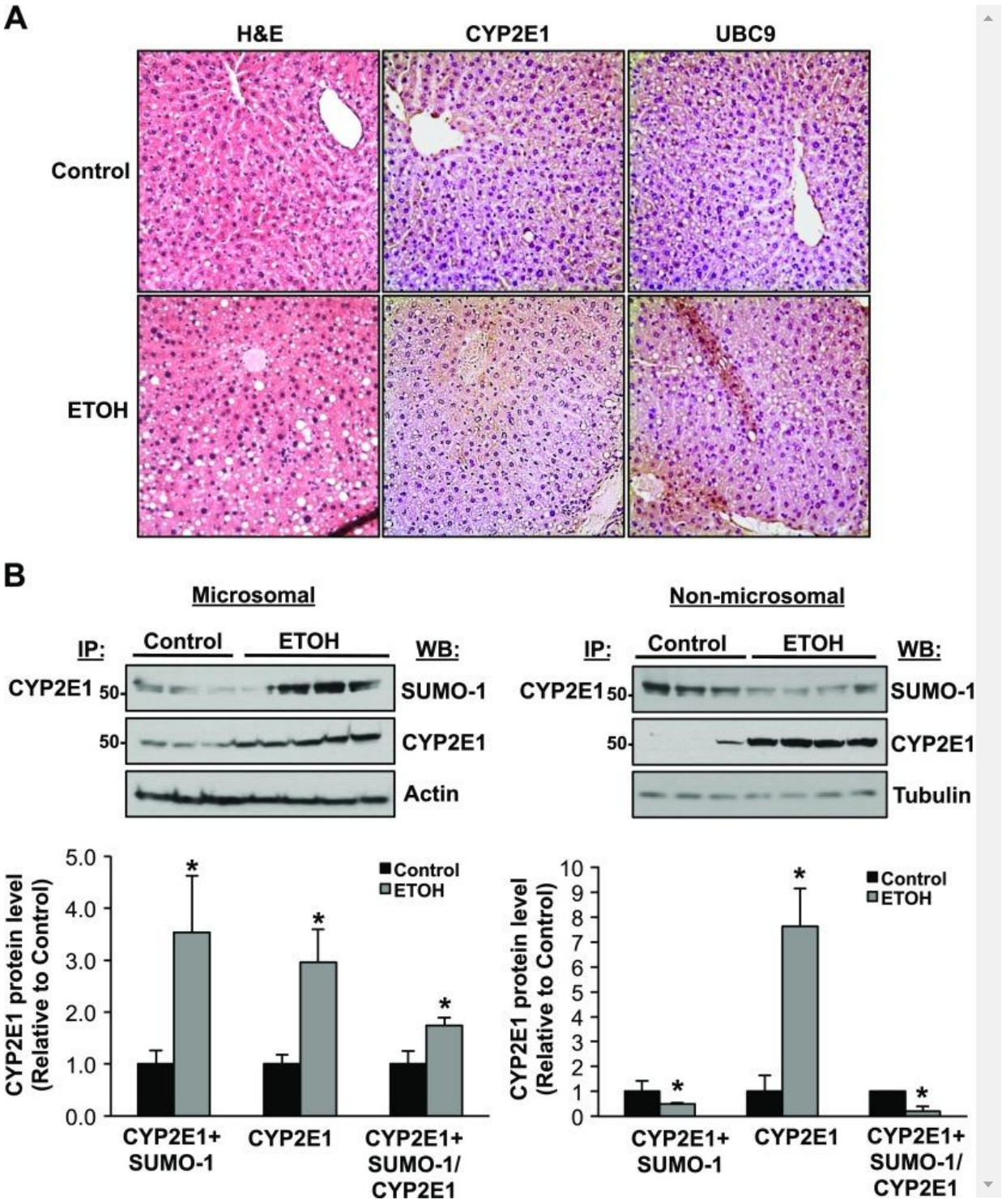

Open in a separate window

SUMOylation regulates CYP2E1 protein trafficking in NIAAA ethanol-binge mouse model. *A*) Immunohistochemical analysis of CYP2E1 and UBC9 expression in ethanol-fed mice. Note positive staining in the centrilobular region. Original magnification, ×20. *B*) Coimmunoprecitation of SUMO-1 and CYP2E1 in ethanol-fed binge mice using 700 μg microsomal and nonmicrosomal proteins. Densitometric ratios normalized to actin are shown in the lower panel. Results are expressed as fold of control (mean ± SEM) from 3–4 mice per group. *$P < 0.05$ *vs.* Sc (microsomal proteins), *$P < 0.04$ *vs.* control (nonmicrosomal proteins).

Figure 4.

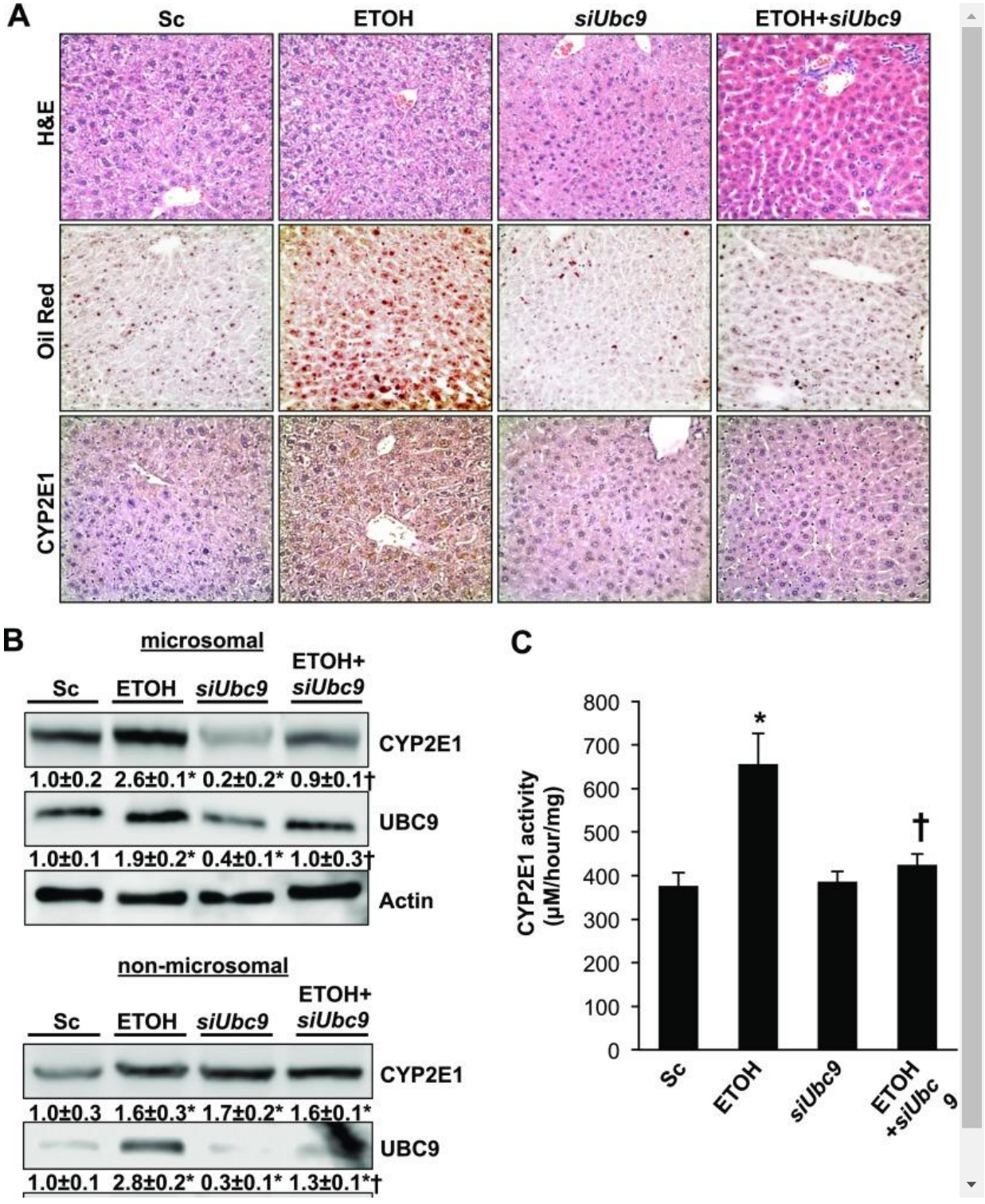

Open in a separate window

UBC9 regulates CYP2E1 protein level, CYP2E1 activity, and triglyceride accumulation in acute ethanol-fed mice. *A*) Immunohistochemical analysis of CYP2E1 and UBC9 expression in acute ethanol-fed mice. Oil red was used to analyze triglycerides. Note positive staining of CYP2E1 and UBC9 in the centrilobular region; ethanol increased their protein levels. Original magnification, ×20. *B*) Microsomal and nonmicrosomal proteins were extracted from liver, and Western blot was performed to measure CYP2E1 protein level. Results are expressed as fold of control (mean ± SEM) from 5–6 mice per group. *$P < 0.04$ *vs.* Sc, †$P < 0.03$ *vs.* ethanol for microsomal proteins, *$P < 0.05$ *vs.* Sc; †$P < 0.05$ *vs.* ethanol for nonmicrosomal proteins. *C*) Liver microsomal CYP2E1 activity was calculated by nitrophenol formation by the incubation time and microsomal protein content (nmol/min/mg). Values are expressed as means ± SEM ($n = 6$). *$P < 0.02$ *vs.* Sc, †$P < 0.02$ *vs.* ethanol

Figure 5.

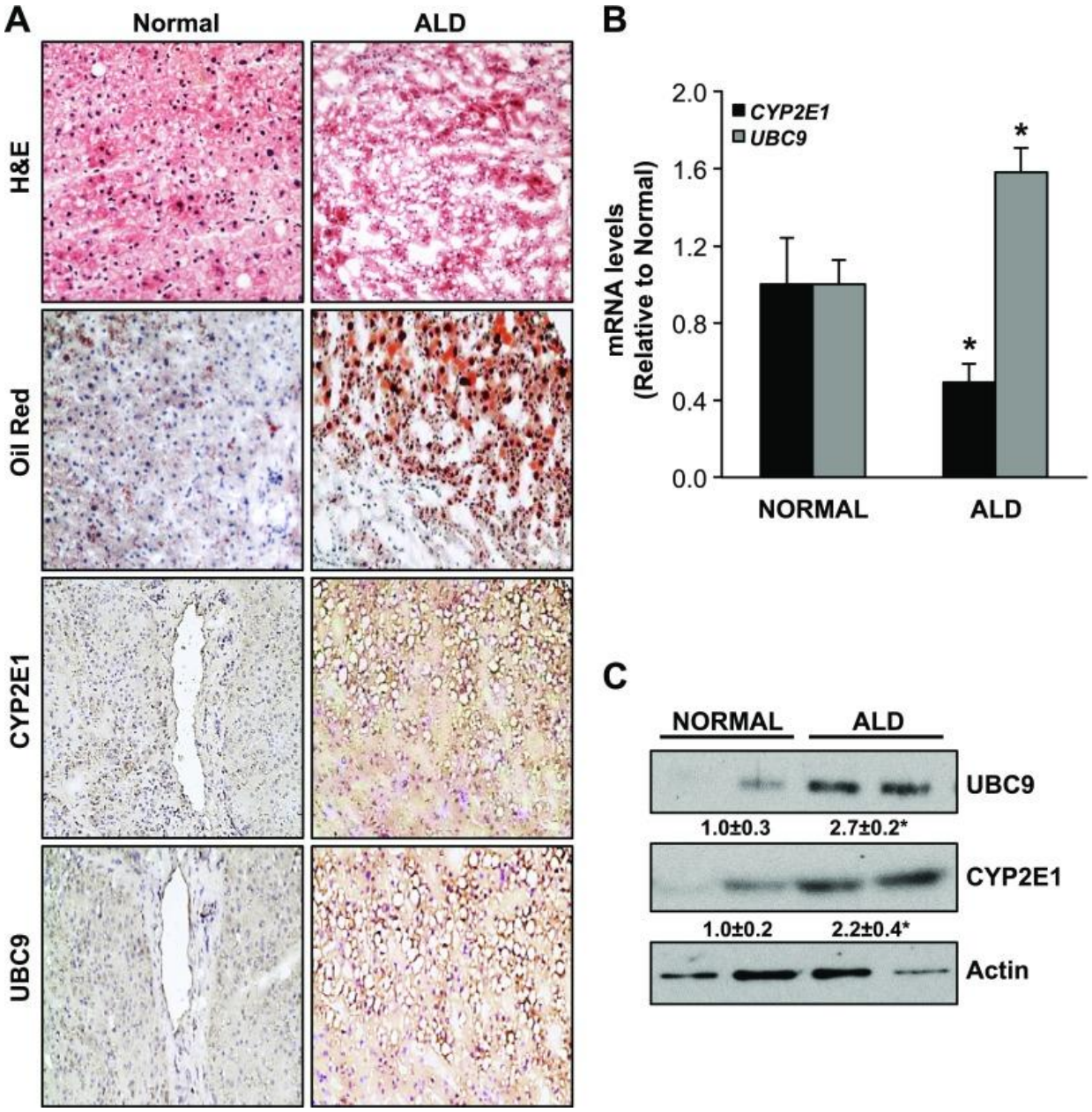

Open in a separate window

UBC9 is overexpressed in human ALD specimens. *A*) Immunohistochemical staining of triglycerides by Oil Red, CYP2E1, and UBC9 proteins in human liver tissues. All hematoxylin and eosin staining or immunochemical staining were shown as typical fields from 5 cases of human normal and 5 alcoholic cirrhosis liver tissues. ALD tissues showed higher levels of UBC9 and CYP2E1 compared with normal tissues. *B*, *C*) CYP2E1 and UBC9 expression. Results are expressed as fold of normal (means ± SEM) from 5 cases of human normal and 5 alcoholic cirrhosis liver tissues. *B*) $*P < 0.03$ *vs.* normal. *C*) $*P < 0.02$ *vs.* normal.

Figure 6.

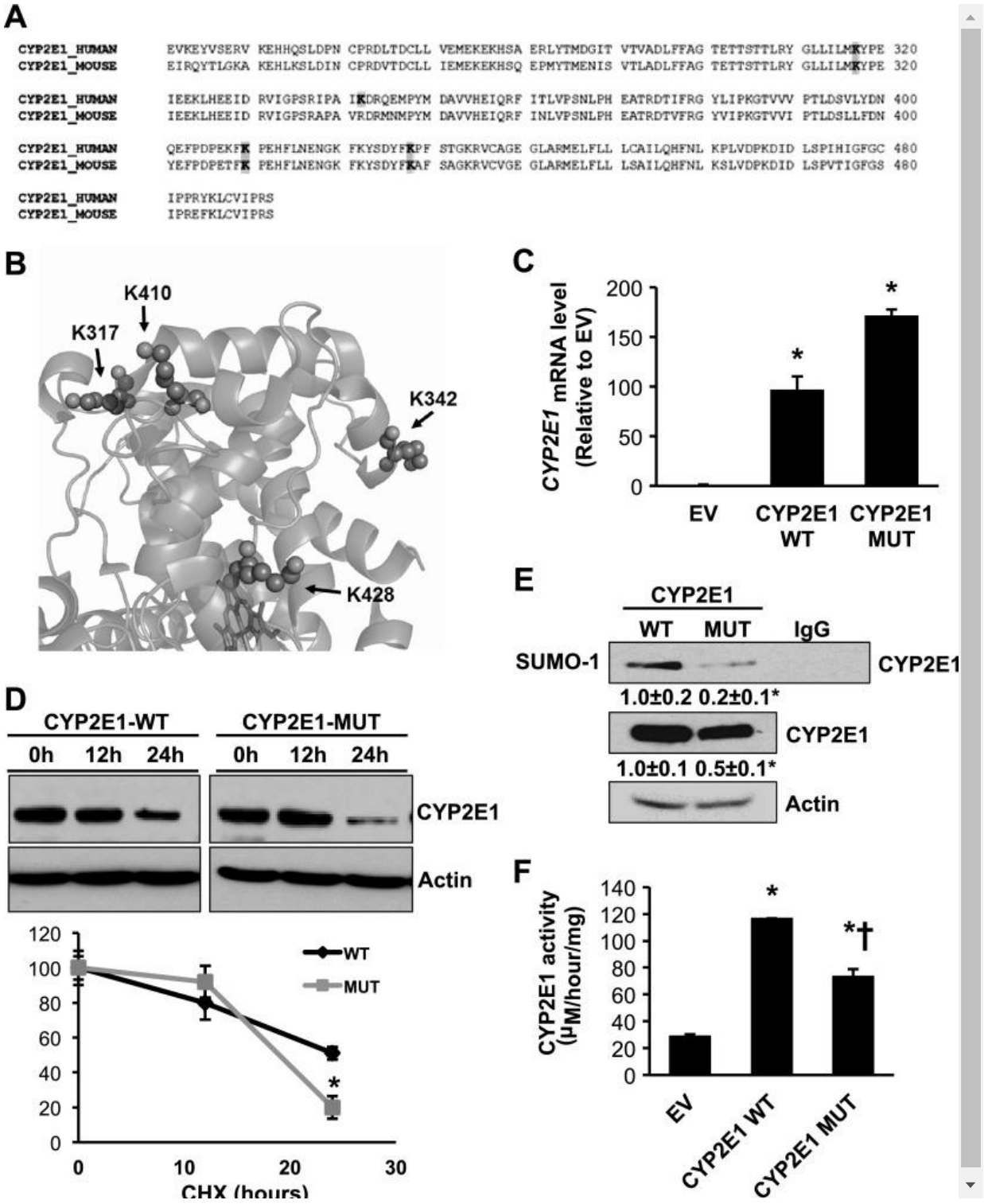

Open in a separate window

SUMOylation of K410 is critical for CYP2E1 protein stability and activity in HepG2 cells. *A*) Human and mouse sequence alignment of CYP2E1. Amino acid residues are colored (gray) based on sequence conservation and similarity between the 2 species. *B*) Three-dimensional crystal structure of CYP2E1 showing all 4 candidate lysine residues for SUMOylation. *C*) HepG2 cells were transfected with CYP2E1-WT or CYP2E1-MUT (A410 mutant) for 12 and 24 h. RNA was extracted and subjected to quantitative real-time PCR analysis with *CYP2E1* TaqMan probe, using *18SrRNA* as housekeeping. Results are expressed as fold of empty vector (EV) (mean ± SEM) from 3 independent experiments. **P* < 0.001 *vs.* EV. *D*) Cells were transfected as in (*C*), and CYP2E1 protein stability was determined by Western blot analyses of DDK tag after cycloheximide (CHX, 5 μg/ml) pretreatment. Representative blots are shown. Protein stability was determined using linear regression (*D*, right panel). Results represent mean ± SEM from 3 independent experiments expressed as percentage of respective 0 h level (*P* < 0.03 between WT and MUT). *E*) SUMO-1 immunoprecipitation of microsomal HepG2 proteins overexpressing WT and mutant CYP2E1 A410 for 24 h. Results are expressed as fold of WT

(means ± SEM) from 3 independent experiments. *$P < 0.01$ *vs.* WT. *F*) HepG2 cell microsomal CYP2E1 activity was calculated by nitrophenol formation incubation time and microsomal protein content (nmol/min/mg). Values are expressed as means ± SEM ($n = 3$). *$P < 0.001$ *vs.* EV, $^{\dagger}P < 0.01$ *vs.* CYP2E1 WT.